Journal of Alloys and Compounds 509 (2011) 451–456

Contents lists available at ScienceDirect

Journal of Alloys and Compounds

journal homepage: www.elsevier.com/locate/jallcom

Enhanced electromagnetic characteristics of carbon nanotubes/carbonyl iron powders complex absorbers in 2–18 GHz ranges

Guoxiu Tong[a,b,*], Wenhua Wu[a], Qiao Hua[a], Yuqing Miao[a], Jianguo Guan[b], Haisheng Qian[a]

[a] College of Chemistry and Life Sciences, Zhejiang Key Laboratory for Reactive Chemistry on Solid Surface, Zhejiang Normal University, Jinhua 321004, PR China
[b] State Key Laboratory of Advanced Technology for Materials Synthesis and Processing, Wuhan University of Technology, Wuhan 430070, PR China

ARTICLE INFO

Article history:
Received 4 June 2010
Received in revised form 9 September 2010
Accepted 9 September 2010
Available online 22 September 2010

Keywords:
Carbon nanotube/iron particle composite
Electrical conductivity
Electromagnetic characteristics
Electromagnetic-wave absorbing property

ABSTRACT

The electromagnetic (EM) characteristics of the carbon nanotubes/carbonyl iron powders (CNTs/CIPs) complex absorbers synthesized by mixing CNTs with CIPs were studied at 2–18 GHz, for the aim of the absorbing coating with thinness, lightness, width, and strength. Compared with CIPs, the CNTs/CIPs composites had higher electrical conductivity, permittivity, and dielectric loss, which gradually increased with the increasing CNTs content (W_{CNTs}). Among them, with W_{CNTs} = 2.2 %, a reflection loss (R_L) exceeding −20 dB was obtained in the frequency range of 6.4–14.8 GHz for a coating thickness of 1.2–2.5 mm. Particularly, a minimum R_L of −33.3 dB was found at 11.2 GHz corresponding to a matching thickness of 1.5 mm. The excellent EM-wave absorption properties are a consequence of a proper EM matching and enhanced absorption abilities resulting from the addition of a small quantity of CNTs with high electrical conductivity, permittivity, and dielectric loss. Thus, CNTs/CIPs complex absorbers may be promising candidates for EM-wave-absorption materials with strong-absorption, thin-thickness, light-weight, and low-cost.

1. Introduction

In recent years, serious EM interferences deriving from the wide applications of electrical and electronic devices in industrial, commercial, and military fields have attracted great interest in exploiting the new EM-wave absorbing materials [1–3]. Hereinto, carbonyl iron powders (CIPs) have been widely used as conventional EM-wave absorbing materials due to their low price, high specific saturated magnetization, and Snoek's limit [4–8]. However, unavoidable disadvantage of overweight makes them very difficult to meet the need of lightness for the absorption coating. Obviously, decreasing the filling fraction can overcome the above disadvantage of overweight, but it always works at the cost of the EM parameters and EM loss. Therefore, when the filling fraction (or the areal density) is reduced, the enhancement of EM matching and absorbing characteristics is of significance. However, the modulation of the permeability in a large scale still is a ticklish problem all over the world. To this end, much recent effort has been devoted to the improvement of EM parameters and the design of coating structures. In comparison with the single-layer absorption coatings, the multi-layer absorption coatings with special structures can significantly enhance the matching and absorbing properties, but their complicated structures generally not only raise the cost but also present the construction technology with difficulties. By contrast, the adjustment of the EM parameters by employing hybrid-type absorbers and/or mixed-type absorbers can conveniently achieve the single-layer absorbing coatings with excellent absorbing properties and simplicity workmanship [5,8]. Until now, some compounding techniques, including mixing, coating, and alloying, were applied to fabricate complex absorbents, such as the composite of magnetic loss absorber and EM-wave-transparent materials (e.g., Fe/SiO_2 [5–8], Fe/Al_2O_3 [9], Fe/ZnO [10]), the magnetic loss/dielectric loss complex absorber (e.g., FeNiMo/C nanocapsules [11], Fe–Ni alloy/C nanotubes [12], Fe/C nanotubes [13]), and the magnetic loss/magnetic loss complex absorber (e.g., Fe/Ni [14], Fe/Fe_2O_3 [15], Fe powders/Fe nanofibers [16]). Among them, the insulating nanomaterials (e.g., SiO_2, Al_2O_3, ZnO, etc.) with low permittivity, on the surface of the metallic iron particles, can suppress the eddy current loss [7,8]. This may expand the effective bandwidth at the expense of the low-frequency absorption properties. Whereas, the combination of magnetic and dielectric materials (e.g., C) in one nanocapsule may generate the high dielectric constant and loss due to effective interface between magnetic and dielectric materials [11–13]. Notwithstanding, this will reduce the weight fraction of magnetic loss absorber and enhance low-frequency absorption properties, complex

* Corresponding author at: College of Chemistry and Life Sciences, Zhejiang Key Laboratory for Reactive Chemistry on Solid Surface, Zhejiang Normal University, Jinhua 321004, PR China. Tel.: +86 579 82282269; fax: +86 579 82282269.
E-mail address: tonggx@zjnu.cn (G. Tong).

0925-8388/$ – see front matter © 2010 Elsevier B.V. All rights reserved.
doi:10.1016/j.jallcom.2010.09.055

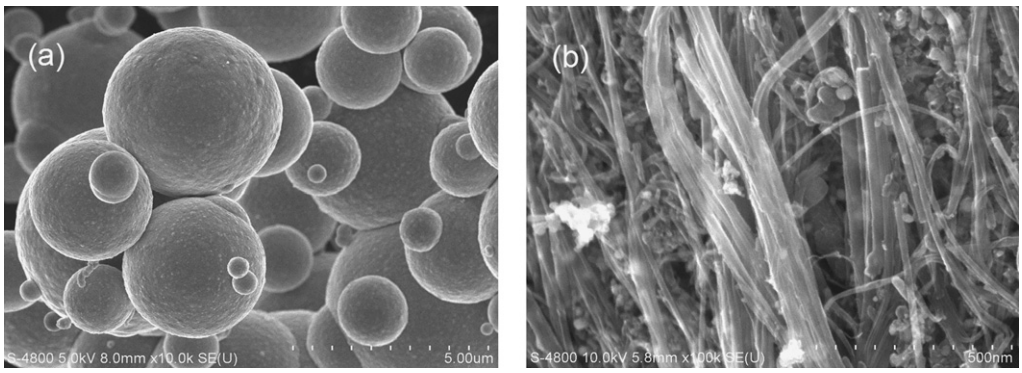

Fig. 1. SEM images of the CIPs (a) and the CNTs (b).

synthetic procedures and special instruments used in the preparation of these complex absorbents usually limit their practical applications.

In this work, decreasing the filling fraction from 40 vol% to 35 vol% and keeping the permeability almost unchanged, the absorption properties can be improved by mixing a small quantity of carbon nanotubes of low density and high permittivity with CIPs, thanks to the enhanced dielectric constant and loss in a proper range. By comparison with the reported literatures [11–13], the excellent absorbing coating materials were prepared by the mixing technique instead of the complicated chemical methods, including the chemical vapor deposition, the catalytic pyrolysis method, or the arc discharge technique. Obviously, the method reported here is more concise and efficient. Thus, it provides an effective approach for the improvement of the conventional absorbing materials and guidance for the design and preparation of thin, light, wide, and strong absorption coating.

2. Experimental

All reagents, such as carbonyl iron powders (CIPs) and carbon nanotubes (CNTs) were obtained from commercial suppliers and were used without any further purification. The morphologies of the aforesaid raw materials were further characterized by SEM. From Fig. 1a, it was clearly observed that the CIPs with the average diameter of 2–3 μm and the relatively smooth surface were composed of a mass of the nanoparticles, whereas, the CNTs with 10–20 μm in length and ca. 50 nm in diameter agglomerated into bundle (Fig. 1b). The formation of the bundle is due to van der Waals attraction during synthesis. The CNTs/CIPs complex absorbents were obtained by homogeneously mixing the CIPs with various weight fractions W_{CNTs} (2.2%, 4.4%, and 6.6%) of the CNTs, as shown in Table 1.

Field-emission scanning electron microscope (FE-SEM) images were taken with a Hitachi S-4800 FE-SEM at an acceleration voltage of 5.0 kV. The element mapping distribution of the samples was acquired by a Horbia EX-250 energy dispersive X-ray spectrometry (EDS) operated at 20.0 kV, associated with FE-SEM. The dc electrical conductivity measurements were made by the standard four-point contact method on pressed rectangular of the CNTs/CIPs composites prepared at room temperature in order to eliminate contact-resistance effects. The transmission/reflection method was applied to determine the relative complex permittivity and permeability of the sample-wax composites through an Agilent N5230 vector network analyzer system. The cylindrical toroidal samples with 3.0 mm in inner diameter, 7.0 mm in outer diameter and 3.5 mm in thickness were fabricated by uniformly mixing wax with 35 vol% CNTs/CIPs composites and then being pressed into cylindrical compacts. Based on the above relative permittivity and permeability at the given frequency, the reflection loss (R_L) curves are calculated according to the equations [17] R_L (dB) = $20\log|(Z_{in}-Z_0)/(Z_{in}+Z_0)|$, where $Z_0 = \sqrt{\mu_0/\varepsilon_0}$ is the characteristic impedance of free space, and the input impedance at free space and materials interface $Z_{in} = Z_0\sqrt{\mu/\varepsilon}\tanh[j(2\pi fd/c)\sqrt{\mu/\varepsilon}]$ is a function of six characteristic parameters, viz. μ', μ'', ε', ε'', f (frequency), and d (the coating thickness).

3. Results and discussion

3.1. Morphology

For better understanding the influence of the W_{CNTs} on morphology of the CNTs/CIPs composites, we investigated the micro-structure and C element mapping distribution of the CNTs/CIPs complex absorbers with various W_{CNTs} by SEM and EDS, respectively. From Fig. 2a and d, it could be seen that the CNTs were heterogeneously dispersed in CIPs matrix with W_{CNTs} = 2.2%, in which CNTs still aggregated into large bundles. Seen from Fig. 2b and e, the percolating network appeared only in a small area with W_{CNTs} = 4.4%. Further increasing W_{CNTs} to 6.6% caused the full formation of percolating network (Fig. 2c and f).

3.2. Electrical conductivity

The dc conductivity (σ) of CNTs/CIPs composites is listed in Table 1 as a function of the weight fraction (W_{CNTs}) of CNTs. The conductivity of the CNTs is ca. 100.50 S cm^{-1}, which is three orders of magnitude higher than that (0.049 S cm^{-1}) of the CIPs. In general, the electrical conductivity of the insulating materials can be improved by adding CNTs owing to its lightweight, high specific surface areas, low percolation, and high electrical property [18,19]. Observed from Table 1, after the 2.2% CNTs with high conductivity are added, the σ of CNTs/CIPs composites slightly increases to 0.068 S cm^{-1}. Also, It is observed that the σ of CNTs/CIPs composites increases by nearly two orders of magnitude at W_{CNTs} = 4.4%. The σ of CNTs/CIPs composites further increases by nearly three times from 4.18 to 13.54 (S cm^{-1}) as we vary W_{CNTs} from 4.4% to 6.6%.

The aforesaid conductive behavior can be interpreted as follows: the conduction mechanism of the CNTs/CIPs composites may be classified mainly into two types. One is ohmic conduction due to the metallic contact between CNTs bundles and CIPs as well as among the CIPs and, the other is non-ohmic conduction owing to existing

Table 1
Conductivity (σ) and EM-wave absorption characteristics of CNTs/CIPs composites with various W_{CNTs}.

W_{CNTs} (%)	Conductivity	EM-wave absorption characteristics			
	σ (S cm^{-1})	Minimum R_L value (dB)	d_m (mm) (R_L < −20 dB)	f_m (GHz) (minimum R_L)	Frequency range (GHz) (R_L < −20 dB)
0	0.049	−22.5	1.2–1.5	14.0	13.6–18.0
2.2	0.068	−33.3	1.2–2.5	11.2	6.4–14.8
4.4	4.18	−41.7	1.8–4.0	4.0	2.8–7.2
6.6	13.54	−12.4	0	2.8	0

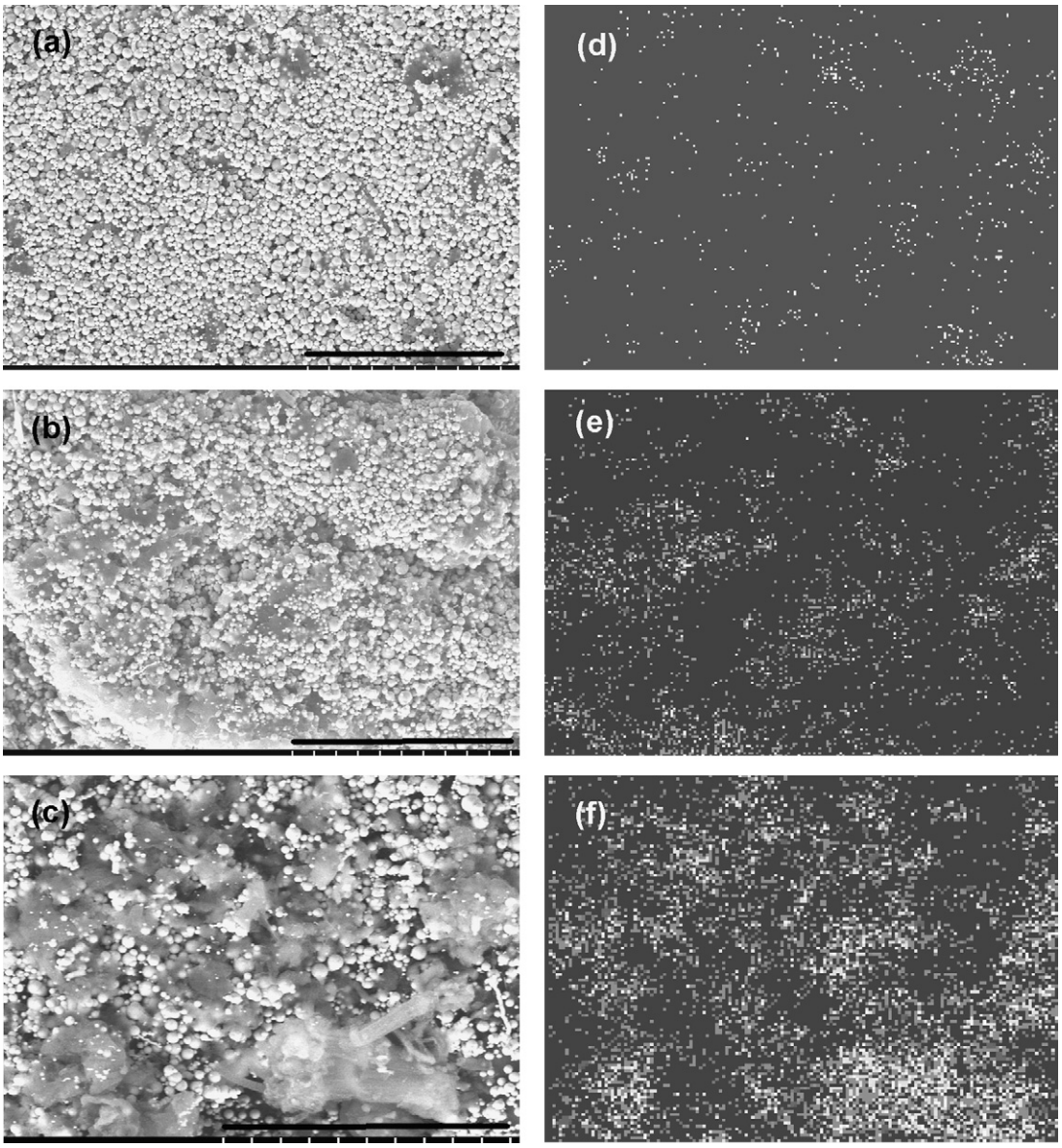

Fig. 2. Microstructure (a–c) and the corresponding C element mapping distribution (d–f) of CNTs/CIPs complex with different W_{CNTs} of: (a and d) 2.2 %; (b and e)) 4.4 %; and (c and f)) 6.6 %. The scale bars in a–c are 100 μm.

small gaps between the CNTs bundles. At the relatively low W_{CNTs} (e.g., 2.2 %), the increasing conductivity of the CNTs/CIPs composites principally depends on the ohmic conduction between CNTs bundles and CIPs. Up to 4.4 %, the gap between the adjacent CNTs bundles significantly decreases and even, the conductive network locally forms (Fig. 2b and e). This arouses an abrupt augment in the σ of the CNTs/CIPs composites under conduction mechanism of non-ohmic conduction. Seen from the SEM images and C element mapping distribution of the CNTs/CIPs composites (Fig. 2c and f), the conductive percolating network basically forms at W_{CNTs} = 6.6 %. This thus causes a further increase in the σ of CNTs/CIPs composites. According to the percolation theory [20], the composites show the percolation behavior with the percolation limit of ca. 6.6 % loading attempted here. The conductivity behavior of the composites is known to be largely dependent upon interaction between the CNTs and CIPs matrix, the properties of the CNTs themselves (diameter, length, specific surface area, and surface conductivity), and the dispersion and the relative concentrations of the CNTs within the matrix.

3.3. Permittivity and permeability

The complex permittivity ($\varepsilon = \varepsilon' - j\varepsilon''$) and permeability ($\mu = \mu' - j\mu''$) determine the storage capability and the loss of the electromagnetic energy and thus play a key role in the EM-wave absorption properties of the coating. As for the ideal absorption coating, the EM parameters must satisfy both the matching and the attenuating. In other word, EM parameters must meet the equation $\mu \approx \varepsilon$ in a wide frequency range and the dielectric loss $tg\delta_E = \varepsilon''/\varepsilon'$ and magnetic loss $tg\delta_M = \mu''/\mu'$ are as large as possible [21]. Only so can the EM-wave enter the coatings to its limit and subsequently be quickly attenuated inside the coatings. For this purpose, such factors as EM parameters, volume fraction, frequency, and coating thickness, should synthetically be taken into account. However, in this study, EM parameters can be controlled only by mixing a small amount of CNTs with CIPs.

The influences of W_{CNTs} on the EM parameters of the wax composites with 35 vol% CNT/CIPs complex absorbent were systematically investigated, as shown in Fig. 3. As for wax composite

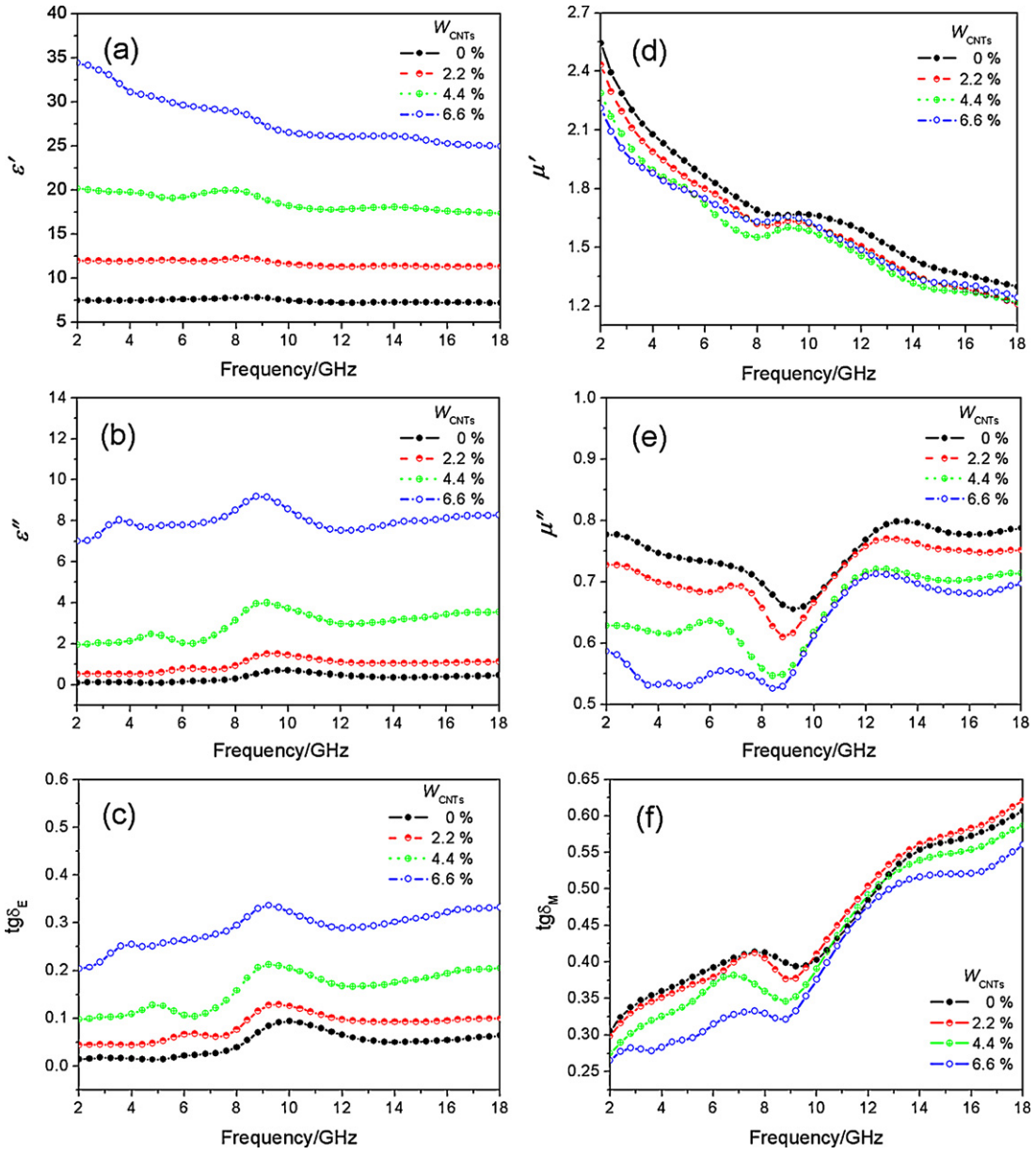

Fig. 3. Influence of W_{CNTs} on the EM parameters for the wax-composites including 35 vol% CNTs/CIPs complex absorbents. (a) The real part ε' and (b) imaginary part ε'' of the permittivity and (c) dielectric loss $tg\delta_E$. (d) The part μ' and (e) imaginary part μ'' of the permeability and (f) magnetic loss $tg\delta_M$.

only including 35 vol% CIPs, the ε' and ε'' are almost constant over 2–18 GHz range ($\varepsilon' = 7.5$ and $\varepsilon'' = 0.2$). When the volume fraction of the absorbent remains the same (35 vol%), increasing W_{CNTs} from 2.2 % to 6.6 % causes a noticeable increase of the ε', ε'', and $tg\delta_E$, for wax composites containing CNTs/CIPs complex absorbents (Fig. 3a–c). Among them, when W_{CNTs} is relatively low (e.g., 2.2 %), ε', especially for ε'' and $tg\delta_E$, are slightly increased. Whereas, with $W_{CNT} = 4.4$ %, there is a sharp rise in ε', ε'' and $tg\delta_E$. Further increasing W_{CNT} to 6.6 %, ε', ε'' and $tg\delta_E$ are significantly augmented and around 4–5, 20–30, and 5–8 times as many as the CIPs', respectively. It suggests that the CNTs/CIPs complex absorbents may have the higher storage capability and the more loss of the electric energy than CIPs, moreover, which increases with the increase of W_{CNTs}.

The aforesaids results can be explained by the following facts: the complex absorbent is composed by CIPs and CNTs. The former is a ferromagnetic matter with both high magnetic loss and low dielectric loss, and the dielectric loss depends on the orientation polarization and interfacial polarization of the inherent electric dipole under the electric field [16]. Whereas the latter is a high dielectric loss matter, in which the mechanisms of dielectric loss include conductance loss ($tg\delta_c$), dielectric relaxation loss ($tg\delta_{rel}$), resonance loss ($tg\delta_{res}$), and other [22,23]. According to the equation $tg\delta_c = 1.8 \times 10^{10}(\sigma/f\varepsilon_r)$ [24], the conductance loss rests upon the electrical conductivity σ, deriving from migrating conductance in the graphite plane direction and the hopping conductance among disordered graphite layers [25,26]. In view of the above-mentioned σ (Table 1), obviously, under the relatively low W_{CNT} (e.g., 2.2 %), the increasing dielectric loss of complex absorbents is ascribed to the high dielectric relaxation loss ($tg\delta_{rel}$) and resonance loss ($tg\delta_{res}$) of carbon nanotubes. However, under the relative high W_{CNT} (e.g., 6.6 %), the soaring dielectric loss of complex absorbents, besides the above reason, is more indebted to the high conductance loss ($tg\delta_c$). It is due to the fact CNTs with the 1D hollow nanostructure, low density and percolation threshold, are prone to form the electric network in the matrix [27]. This indicates that ε', ε'' and $tg\delta_E$ can be facilely modulated by homogeneously mixing a small

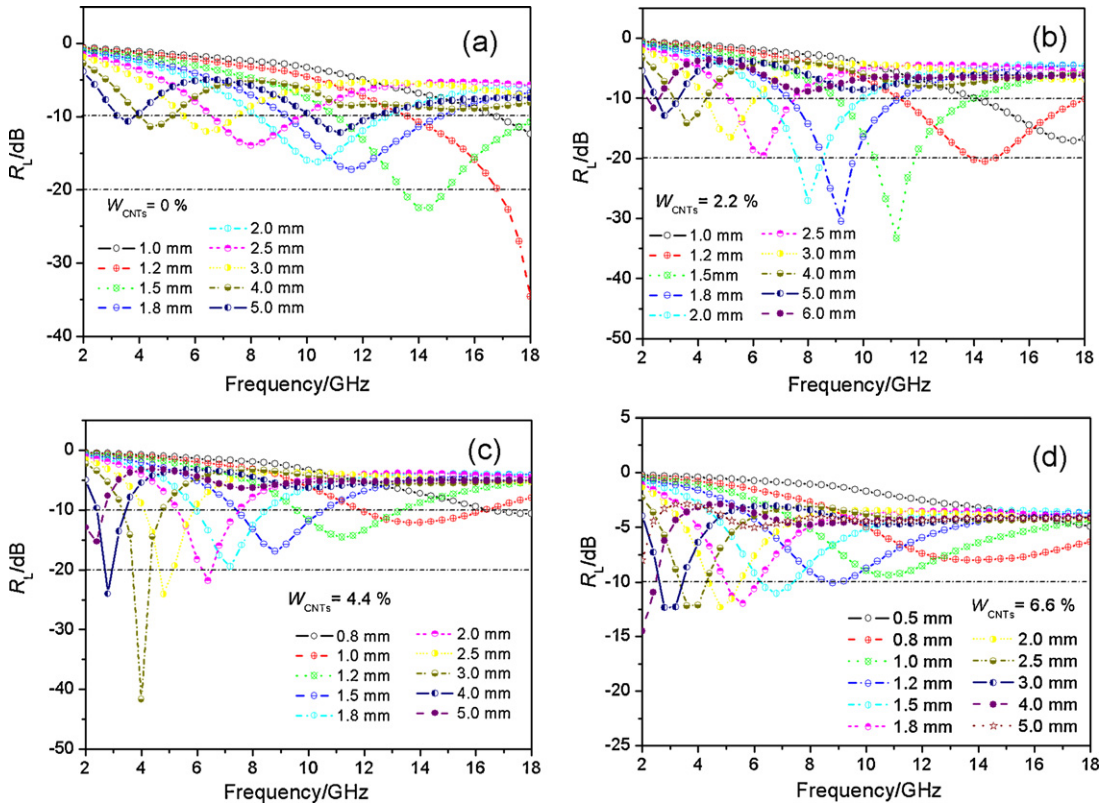

Fig. 4. Calculated reflection loss (R_L) curves versus frequency f of the coatings with different coating thicknesses containing the wax-composites including 35 vol% CNTs/CIPs complex absorbers with various W_{CNTs}.

quantity of CNTs with CIPs within a proper range. In addition, the two strong resonance peaks corresponding to ε'' at 3–5 GHz and 8–10 GHz, respectively, enhance with increasing W_{CNT}, thanks to resonance loss ($tg\delta_{res}$) of carbon nanotubes.

Fig. 3d–f shows that for the CIPs-wax composites, the μ' gradually decreased owing to the domain-wall motion and relaxation as the frequency increase [28] and the μ'' values varied from 0.6 to 0.8. Obviously, this is higher than ε'' (Fig. 3b), implying the poor matching properties. Meanwhile, two resonance peaks could be observed at 7.0 GHz and 13 GHz on the μ'' plots, respectively. Usually, for ferromagnetic materials there are two types of magnetic resonances, including ferromagnetic and spin resonances. The former normally emerges at low frequency region (<2 GHz) owing to domain wall motion, while the latter appears at high frequency region due to spin rotational component [29]. The similar multi-resonance behavior was also observed for metallic magnetic particles and carbon-coated iron nanocapsules [30]. This is defined as "exchange mode" resonance, a consequence of the small size effect, surface effect and spin wave excitations. Apparently, in this study, the first resonance peak (around 7 GHz) may be ascribed to the "exchange mode" resonance benefiting from the addition of the CNTs with high conductivity. Whereas the second resonance peak (around 13 GHz) may be associated with natural resonance.

When a small amount of CNTs (e.g., 2.2 %) was mixed with CIPs, the corresponding μ' and μ'' for CNTs/CIPs wax composites slightly decreased and the magnetic loss $tg\delta_M$ showed less variation. Additionally, it is observed that μ'' is closest to ε'' (Fig. 3b), indicating the best matching characteristics. Increasing W_{CNTs} to 4.4 % leads to a gradual decrease in μ', μ'', and $tg\delta_M$ for CNTs/CIPs wax composite, owing to the decreasing content of ferromagnetic CIPs [31]. However, further increasing W_{CNTs} to 6.6 %, the appearances of significant fluctuations are μ', μ'' and $tg\delta_M$. Generally, the magnetic loss of CNTs/CIPs composites, involving eddy current loss, magnetic hysteresis loss, and residual loss, mostly depends on the weight fraction of ferromagnetic CIPs. However, according to the eddy current loss coefficient $e = 4\pi^2\mu_0 d^2\sigma/3$, the high electric conductivity may make the permeability of the CNTs/CIPs wax composites unstable, and then limits its high frequency application [32]. The above results demonstrate that permeability parameters can also be adjusted in a small range by mixing CNTs with CIPs.

3.4. EM-wave absorption performance

To further reveal the influence of W_{CNTs} on the EM-wave absorption properties, reflection loss (R_L) of the wax composite including 35 vol% CNTs/CIPs complex absorbers was calculated according to the transmit-line theory [17]. From Fig. 4, firstly, all R_L curves were found to gradually shift to lower frequency with the increasing coating thickness. Secondly, the minimum R_L value changed with the coating thickness, which was in accord with the relationship between the matching thickness (d_m) and the matching frequency (f_m) corresponding to the eq. $d_m = c/(4f_m\sqrt{|\mu||\varepsilon|})$, where c is the velocity of light. As for the CIPs (Fig. 4a), the R_L values (below −20 dB) were obtained in 13.6–18.0 GHz, with thickness of 1.2–1.5 mm, while the minimum R_L value was −22.5 dB at 14 GHz corresponding to a 1.5 mm matching thickness. When the volume fraction (35 vol%) of the absorber kept unchanged, the addition of CNTs begot a significant change in the EM-wave absorption property of CNTs/CIPs composites. Thereinto, with W_{CNT} = 2.2 %, a minimum R_L value of −33.3 dB was observed at 11.4 GHz on a coating with a matching thickness of 1.5 mm. While the absorption range under −10 dB was over 2.4–18 GHz frequency range (Fig. 4b). Increasing W_{CNTs} to 4.4 %, it was found that the R_L peak value of CNTs/CIPs wax composites reached a minimum of −41.7 dB at 4 GHz with regard to a 3.0 mm matching thickness

(Fig. 4c). Moreover, the absorption range under −10 dB was in the whole frequency range (2–18 GHz). This indicates that the aforesaid CNTs/CIPs composites are excellent absorber with strong-absorption and broad-bandwidth. However, further elevating W_{CNT} to 6.6 %, the minimum R_L was no more than −12.4 dB at 2.8 GHz with a matching thickness of 3.0 mm (Fig. 4d). The significantly decreasing EM-wave absorbing properties are mainly ascribed to the exorbitant permittivity originating from the full formation of percolating network. It arouses the serious mismatching between the free space impedance Z_0 and the input impedance Z_{in} and thus inhibits the incidence waves into the absorbing coating.

The EM-wave absorption properties of CIPs and CNTs/CIPs wax composites were summarized in Table 1. A comparison of the CNTs/CIPs complex absorbers with CIPs showed that when the coating thickness remained the same, the minimum R_L point moved toward the lower frequency region. It implied that CNTs/CIPs complex absorbers could have better low-frequency absorbing properties. This shift is attributed to the high dielectric constant and dielectric loss, resulting from one-dimensional hollow structures with the large specific surface area and shape anisotropism. While, as for a close effective bandwidth (ca. 7 GHz, <−10 dB), CNTs/CIPs complex absorbers had thinner matching thickness (1.2 mm) than CIPs (1.5 mm) (Fig. 4a–b). Meanwhile, the maximum attenuation (−33.3 dB) of the incident wave corresponding to the CNTs/CIPs complex absorbers was conspicuously higher than that (−17.2 dB) of CIPs owing to the strong resonance behavior. Additionally, the EM-wave absorption bandwidth of CNTs/CIPs complex absorbers, with R_L < −20 dB, was broadened from 4.4 to 8.4 GHz range compared with CIP (Table 1). The above results demonstrated that the coating containing CNTs/CIPs complex absorbers W_{CNT} 2.2 % would have thinner thickness, stronger absorption, and broader bandwidth than CIPs absorption coating. It is due to the fact that the addition of a small quantity of CNTs with special one-dimensional structure and high surface area can effectually improve the EM matching and absorbing properties.

Furthermore, it is worth noting that the R_L values (<−20 dB) are gained in the 6.4–14.8 GHz frequency range, which are broader frequency ranges than those reported in the literature, i.e. Fe/SmO (0.73–1.3 GHz) [33], Fe/Fe_3B/Y_2O_3 (2.7–6.5 GHz) [34], Fe/C (4.4–8.3 GHz) [31], Co filled C nanotubes (15.3–16.5 GHz) [35], Co/C nanotubes [36], (Fe, Ni)/C nanocapsules (13.6–16.6 GHz) [37], Fe-filled C nanotubes (15.3–16.2 GHz) [38], γ-Fe_2O_3-multiwalled carbon nanotubes (MWCNT) and Fe/Fe_3C-MWCNT [39], and carbon nanotubes/$CoFe_2O_4$ spinel nanocomposite [40]. Thus, the R_L values of −20 dB corresponding to the 99 % attenuation of the incident wave can be considered as a powerful absorber in practice utilization.

4. conclusions

CNTs/CIPs complex absorbers were prepared by mixing a small quantity of CNTs of lightweight, high permittivity, and high conductivity with CIPs of high magnetic loss and large density. The investigation of the EM characteristics showed that conductivity, permittivity, and dielectric loss corresponding to the CNTs/CIPs complex absorbers gradually increased with the increasing W_{CNTs}. Thereinto, the wax-composites containing 35 vol% CNTs/CIPs composites with W_{CNTs} = 2.2 % showed excellent EM-wave absorption characteristics with a minimum R_L value of −33.3 dB at 11.4 GHz on a coating with a matching thickness of 1.5 mm and <−20 dB (99 % attenuation of the incidence wave) with thickness of 1.2–2.5 mm in the 6.4–14.8 GHz. The enhanced absorption properties are mainly ascribed to the enhancement of the matching-absorbing abilities. This study suggests that with the permeability unchanged, the light, wide, and strong absorbing coating can be achieved by raising the permittivity constant and dielectric loss within a certain range. Thus, the possible application of producing strong, broad, and light absorbing coating from CNTs/CIPs composites is achievable.

Acknowledgements

This work was supported in part by the National High-Technology Research and Development Program of China (No. 2006AA03A209), National Defense Fundamental Research Project (D1420061057), Natural Scientific Foundation of Zhejiang Province (Project No. Y4100022), New Bud Talents Grant from Zhejiang Province (No. ZC323010035), Doctoral Start-up Foundation from Zhejiang Normal University (No. ZC304009094), and Open Lab Project from Zhejiang Normal University.

References

[1] G.X. Tong, J.G. Guan, Z.D. Xiao, F.Z. Mou, W. Wang, G.Q. Yan, Chem. Mater. 20 (2008) 3535–3539.
[2] X.A. Fan, J.G. Guan, Z.Z. Li, F.Z. Mou, G.X. Tong, W. Wang, J. Mater. Chem. 20 (2010) 1676–1682.
[3] J.R. Liu, M. Itoh, M. Terada, T. Horikawa, K. Machida, Appl. Phys. Lett. 91 (2007) 093101.1–093101.3.
[4] X.A. Fan, J.G. Guan, W. Wang, G.X. Tong, J. Phys. D: Appl. Phys. 42 (2009) 75006–75012.
[5] G.X. Tong, W. Wang, J.G. Guan, Q.J. Zhang, J. Inorg. Mater. 21 (2006) 1461–1466.
[6] X.M. Ni, Z. Zheng, X.K. Xiao, L. Huang, L. He, Mater. Chem. Phys. 120 (2010) 206–212.
[7] X.J. Wei, J.T. Jiang, L. Zhen, Y.X. Gong, W.Z. Shao, C.Y. Xu, Mater. Lett. 64 (2010) 57–60.
[8] X.M. Ni, Z. Zheng, X. Hu, X.K. Xiao, J. Colloid Interface Sci. 341 (2010) 18–22.
[9] G.X. Tong, J.G. Guan, W. Wang, L.Y. Zhao, Chin. J. Mater. Res. 22 (2008) 102–106.
[10] X.G. Liu, D.Y. Geng, H. Meng, P.J. Shang, Z.D. Zhang, Appl. Phys. Lett. 92 (2008) 173117.1–173117.3.
[11] X.G. Liu, Z.Q. Ou, D.Y. Geng, Z. Han, H. Wang, B. Li, E. Brück, Z.D. Zhang, J. Alloys Compd. (2010), doi:10.1016/j.jallcom.2010.07.085.
[12] M.H. Xu, W. Zhong, X.S. Qi, C.T. Au, Y. Deng, Y.W. Du, J. Alloys Compd. 495 (2010) 200–204.
[13] D.L. Zhao, X. Li, Z.M. Shen, J. Alloys Compd. 471 (2009) 457–460.
[14] S. Jia, F. Luo, Y.C. Qing, W.C. Zhou, D.M. Zhu, Phys. B 405 (2010) 3611–3615.
[15] M.J. Park, J. Choi, S.S. Kim, IEEE Trans. Magn. 36 (2000) 3272–3274.
[16] G.X. Tong, J.G. Guan, W.Y. Zhang, W. Zhang, W. Wang, D.M. Dong, Acta Metal. Sin. 44 (2008) 1001–1005.
[17] L.G. Yan, J.B. Wang, Y.Z. Ye, Z. Hao, Q.F. Liu, F.S. Li, J. Alloys Compd. 487 (2009) 708–711.
[18] Y.J. Kim, T.S. Shin, H.D. Choi, J.H. Kwon, Y.C. Chung, H.G. Yoon, Carbon 43 (2005) 23–30.
[19] X.S. Fang, Y. Bando, U.K. Gautam, C.H. Ye, D. Golberg, J. Mater. Chem. 18 (2008) 509–522.
[20] E.J. Garboczi, K.A. Snyder, J.F. Douglas, M.F. Thorpe, Phys. Rev. E 52 (1995) 819–828.
[21] G.X. Tong, J.G. Guan, X.A. Fan, W. Wang, W. Li, Acta Metall. Sin. 44 (2008) 867–870.
[22] X.S. Fang, C.H. Ye, T. Xie, Z.Y. Wang, J.W. Zhao, L.D. Zhang, Appl. Phys. Lett. 88 (2006) 013101.1–013101.3.
[23] X.S. Fang, C.H. Ye, L.D. Zhang, T. Xie, Adv. Mater. 17 (2005) 1661–1665.
[24] H.R. Li, Introduction to Dielectric Physics, Chengdu University of Technology Press, Chengdu, 1990.
[25] B. Reznik, D. Gerthsen, K.J. Hüttinger, Carbon 39 (2001) 215–229.
[26] G.B. Zheng, H. Sano, K. Suzuki, K. Kobayashi, Y. Uchiyama, H.M. Cheng, Carbon 37 (1999) 2057–2062.
[27] Z.F. Liu, G. Bai, Y. Huang, F.F. Li, Y.F. Ma, T.Y. Guo, X.B. He, X. Lin, H.J. Gao, Y.S. Chen, J. Phys. Chem. C 111 (2007) 13696–13700.
[28] S.T. Jiang, W. Li, Condensed Magnetic Matter, Science Press, Beijing, 2003, p. 402.
[29] X. Tang, Q. Tian, B.Y. Zhao, K. Hu, Mater. Sci. Eng. A 445–446 (2007) 135–140.
[30] X.F. Zhang, X.L. Dong, H. Huang, B. Lv, J.P. Lei, C.J. Choi, J. Phys. D: Appl. Phys. 40 (2007) 5383–5387.
[31] H. Bia, K.C. Koua, K. Ostrikovc, L.K. Yan, Z.C. Wang, J. Alloys Compd. 478 (2009) 796–800.
[32] J.R. Liu, M. Itoh, K. Machida, Appl. Phys. Lett. 88 (2006) 062503.1–062503.3.
[33] S. Sugimoto, T. Maeda, D. Book, T. Kagotani, K. Inomata, M. Homma, H. Ota, Y. Houjou, R. Sato, J. Alloy. Compd. 330–332 (2002) 301–306.
[34] J.R. Liu, M. Itoh, T. Horikawa, M. Itakura, N. Kuwano, K. Machida, J. Phys. D: Appl. Phys. 37 (2004) 2737–2741.
[35] H.Y. Lin, H. Zhu, H.F. Guo, L.F. Yu, Mater. Res. Bull. 43 (2008) 2697–2702.
[36] Z. Zheng, B. Xu, L. Huang, L. He, X.M. Ni, Solid State Sci. 10 (2008) 316–320.
[37] X.G. Liu, B. Li, D.Y. Geng, W.B. Cui, F. Yang, Z.G. Xie, D.J. Kang, Z.D. Zhang, Carbon 47 (2009) 470–474.
[38] H.Y. Lin, H. Zhu, H.F. Guo, L.F. Yu, Mater. Lett. 61 (2007) 3547–3550.
[39] P. Xu, X.J. Han, X.R. Liu, B. Zhang, C. Wang, X.H. Wang, Mater. Chem. Phys. 114 (2009) 556–560.
[40] R.C. Che, C.Y. Zhi, C.Y. Liang, X.G. Zhou, Appl. Phys. Lett. 88 (2006) 033105.1–033105.3.